Stability Switches in a Host–Pathogen Model as the Length of a Time Delay Increases

**Jennifer J.H. Reynolds · Jonathan A. Sherratt ·
Andrew White**

Abstract The destabilising effects of a time delay in mathematical models are well known. However, delays are not necessarily destabilising. In this paper, we explore an example of a biological system where a time delay can be both stabilising and destabilising. This example is a host–pathogen model, incorporating density-dependent prophylaxis (DDP). DDP describes when individual hosts invest more in immunity when population densities are high, due to the increased risk of infection in crowded conditions. In this system, as the delay length increases, there are a finite number of switches between stable and unstable behaviour. These stability switches are demonstrated and characterised using a combination of numerical methods and analysis.

1 Introduction

Time delays are an inherent feature of many biological systems, ranging from cell biology to ecology. In many cases the importance of delays lies in their ability to destabilise equilibria. For instance in physiology, increased time delays can lead to

---

J.J.H. Reynolds (✉) · J.A. Sherratt · A. White
Department of Mathematics and the Maxwell Institute for Mathematical Sciences, Heriot-Watt University, Edinburgh EH14 4AS, UK
e-mail: j.j.h.reynolds@dunelm.org.uk

 Springer

'dynamical diseases' such as hematopoiesis and Cheyne–Stokes respiration, in which physiological quantities that are constant in healthy individuals become oscillatory (Mackey and Milton 1987; Fowler and Kalamangalam 2000; Colijn and Mackey 2005). Similarly, the population cycles in Nicholson's classic blowfly experiment are due to time delays associated with development (Nicholson 1954; Gurney et al. 1980; Berezansky et al. 2010).

Mathematical theory shows that time delays are not necessarily destabilising: the introduction of a time delay can stabilise an otherwise unstable equilibrium. Moreover in some cases there can be multiple switches between stability and instability as the delay length is increased (Mufti 1964; Lee and Hsu 1969; Mahaffy 1982; Cooke and van den Driessche 1986; Kuang 1993). However, there are relatively few specific examples of such behaviour. May (1973) described a population model with three stability regions as the time delay increases. Hastings (1983) analysed stability of models of age-dependent predation, and found numerically that any finite number of switches is possible. Multiple stability switches as the delay increases were also reported by Xiao et al. (2009), who extended a host–free-living pathogen model framework by including delayed host self-regulation. Here we demonstrate a new example of the phenomenon, and present a detailed mathematical study, which enables us to make detailed predictions such as the number of stability switches as a function of model parameters.

In this paper, we show and describe multiple stability switching as delay length increases in a host–pathogen system including density-dependent prophylaxis. The maintenance of mechanisms that allow hosts to resist pathogen infection can be costly. For instance, mounting an immune response could involve damaging autoimmune effects (e.g. Råberg et al. 1998). In addition, immune function may be traded off with other traits, such as the ability to compete (Kraaijeveld and Godfray 1997); when immunity levels are high, less resources are available to be allocated elsewhere. Therefore, individuals will benefit from tailoring their allocation of resources to immunity in order to match the perceived risk of exposure to disease. In many cases transmission of pathogens is positively density-dependent (Anderson and May 1979; Ryder et al. 2005, 2007), so that the probability of infection increases with host population density. In such cases there is likely to be a selective advantage to individuals that increase their investment in immunity in response to increasing population density. This phenomenon is termed density-dependent prophylaxis (DDP) (Wilson and Reeson 1998).

DDP has been experimentally demonstrated in a number of insect species. For example, larvae of both the Oriental armyworm *Mythimna separata* and the African armyworm *Spodoptera exempta* show increased viral resistance when reared at high population densities (Kunimi and Yamada 1990; Reeson et al. 1998). Mealworm beetles (*Tenebrio molitor*) reared under crowded conditions show more resistance to a generalist entomopathogenic fungus than those reared singly (Barnes and Siva-Jothy 2000). A similar response has been demonstrated in the desert locust *Schistocerca gregaria* (Wilson et al. 2002). Furthermore, a study on adult bumble-bee workers (*Bombus terrestris*) concluded that there is rapid plasticity in immunity levels dependent on social context (Ruiz-González et al. 2009). This demonstration of DDP in adults suggests that it may be a widespread phenomenon, and considerably broadens its potential significance.

There is a time delay in the onset of DDP, representing the time between the change in population density and the subsequent phenotypic change in the level of resistance. In a previous paper (Reynolds et al. 2011) we have shown that short time delays can stabilise an otherwise unstable equilibrium, therefore reducing the extent of the parameter region giving population cycles. In this paper, we show that increasing the length of the time delay gives multiple switches in stability, resulting in a complex dependence of the population dynamics on demographic parameters. Our host–pathogen model incorporating DDP is introduced in Sect. 2. Next the population dynamical behaviour of the model is explained and illustrated, in Sect. 3. We provide some details in Sect. 4 of the continuation method used to produce the stability boundary curves. Section 5 is an analysis of the observed switches in stability.

2 The Model

The host–pathogen model framework used by Reynolds et al. (2011) to represent DDP is as follows:

$$\frac{dH}{dt} = rH\left(1 - \frac{H}{K}\right) - \alpha Y, \tag{1}$$

$$\frac{dY}{dt} = \beta_0\left(1 - p\frac{H_T}{K}\right)W(H - Y) - (\alpha + b)Y, \tag{2}$$

$$\frac{dW}{dt} = \lambda Y - \mu W, \tag{3}$$

where $H_T := H(t - T)$. This is based on an extension of Anderson and May's (1981) Model G, with self-regulation of the host (Bowers et al. 1993). Here H is the total host population density, within which Y is the density of infected (and infectious) individuals, and X the density of susceptible individuals, such that $H = X + Y$. W is the density of free-living stages of the pathogen population. Throughout this study, we use the differential equation for total host density H, but alternatively one could use the equation for susceptible host density X:

$$\frac{dX}{dt} = (r + b)(X + Y) - bX - r\frac{(X + Y)^2}{K} - \beta_0\left(1 - p\frac{H_T}{K}\right)WX; \tag{4}$$

then the model in terms of X, Y and W consists of Eqs. (2), (3) and (4). The model assumes that host self-regulation acts on birth rate and that both susceptible and infected hosts can die naturally. Susceptible hosts may become infected through contact with free-living infective stages of the pathogen, and then experience additional mortality due to the disease. Infected hosts release infective stages at a constant rate, and these stages are lost through natural decay. Note that this system is confined to the set $0 \le H \le K, 0 \le Y \le H, 0 \le W \le (\lambda/\mu)Y$.

The parameters in the model are all positive. Parameter r is the intrinsic rate of net increase of the host (birth rate minus the natural host death rate b), K is the host

carrying capacity and α is the rate of disease-induced mortality. The term

$$\beta_0\left(1 - p\frac{H_T}{K}\right)$$

gives the transmission coefficient of the disease. Here β_0 is the transmission coefficient of the disease when there is no DDP; p is a measure of the strength of the prophylactic effect (specifically, a proportion, taking a value between 0 and 1); and T is the time delay in the onset of DDP, i.e. the delay between the change in density and the subsequent phenotypic change in resistance level. Note that as $H \leq K$, the transmission coefficient function is always non-negative. Parameter λ is the rate at which an infected host produces infective stages of the pathogen. Finally, μ is the decay rate of the infective stages of the pathogen.

3 Population Dynamics

The model (1)–(3) has three steady states: the trivial state ($H = 0$, $Y = 0$, $W = 0$), which is always unstable since we assume $r > 0$, the disease-free state ($H = K$, $Y = 0$, $W = 0$) and an infected state (H^*, Y^*, W^*) where

$$Y^* = \frac{r}{\alpha}H^*\left(1 - \frac{H^*}{K}\right),$$

$$W^* = \frac{\lambda}{\mu}Y^*$$

and H^* is a solution to the cubic equation

$$\left(H^*\right)^3\left(\frac{pr}{\alpha K^2}\right) - \left(H^*\right)^2\left(\frac{r}{\alpha K} + \frac{pr}{\alpha K} - \frac{p}{K}\right) + H^*\left(\frac{r}{\alpha} - 1\right) + \frac{\mu(\alpha + b)}{\lambda\beta_0} = 0. \quad (5)$$

It should be noted that the solution for H^* may not be unique. Equation (5) always has one negative root, which is not ecologically relevant. The two roots that remain can both be complex, in which case there is pathogen extinction. Otherwise there are two positive, real roots. In most cases, one is less than K and one is greater than K, the latter not being relevant. For some parameters, both roots can be greater than K, so neither is relevant: in this case pathogen extinction occurs. There are also parameter sets for which both roots are less than K and so both are potentially relevant to ecological applications. However, in such cases the larger root corresponds to a steady state that is always unstable. We focus on the smaller of the two roots when this case arises. (This matter is discussed in more detail in Reynolds et al. (2011).)

Our study focuses on the assessment of the stability of the non-trivial steady state (H^*, Y^*, W^*). For certain parameter values this infected state is unstable, and then one expects population cycles of host and pathogen to occur (Anderson and May 1981; Bowers et al. 1993; White et al. 1996). We explore the population dynamical consequences of increasing the delay term (T) in the model. The complex structure of the parameter space giving cycles for long delays is described and discussed.
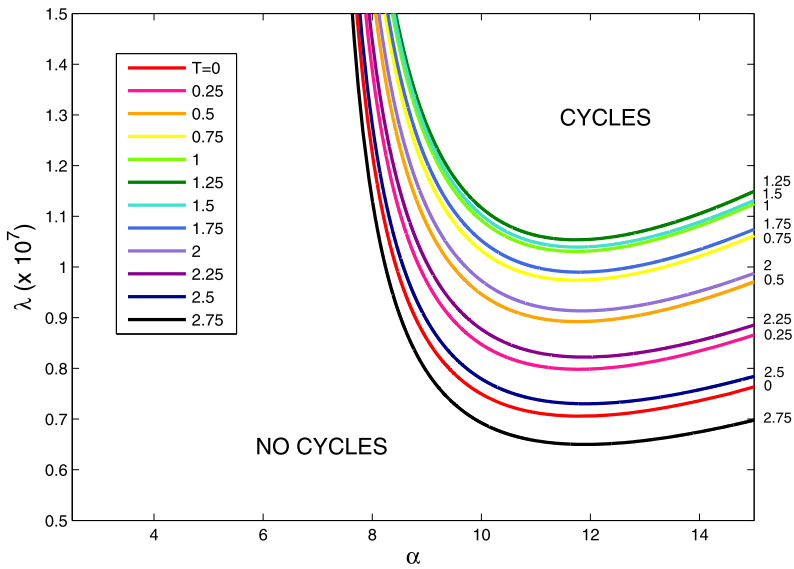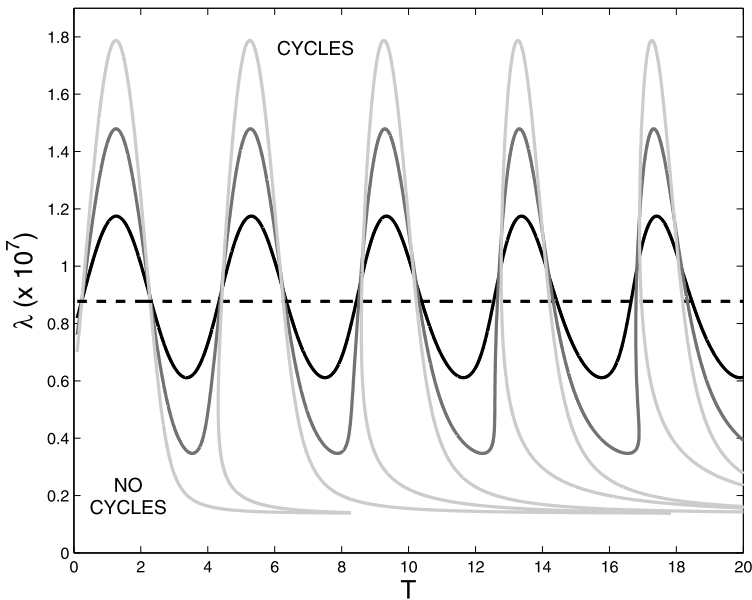
Fig. 1 Stability boundary curves for different T values, for a fixed p ($p = 0.2$), showing that increasing the delay is not consistently stabilising. Delay values are $T = 0 : 0.25 : 2.75$, and an increasing T is represented by a change in colour from *red* to *black* (or from *pale gray* to *black*). As the delay increases, firstly the cycling parameter region diminishes, and then it expands. The stability boundary curves depicted here, and in the other figures in this study, are produced using a numerical continuation method, as described in Sect. 4. The other parameter values, which are the same for all figures in this paper, are: $r = 1$, $K = 1$, $\beta_0 = 0.0001$, $\mu = 3$ and $b = 3.3$

In Reynolds et al. (2011) the implications of DDP were explored for the population dynamics of a host–pathogen system. The delay was found to be critical in determining whether DDP is stabilising or destabilising. In that study, attention was restricted to relatively short delays. In this paper, we explore the dynamical effects of extending the delay beyond this. We find that complex and interesting patterns of dynamical behaviour occur in parameter space with this lengthened delay.

Reynolds et al. (2011) found that increasing the delay reduces the region in parameter space where the solutions are cyclic, and thus stabilises the system. However, with longer delays, increasing the delay is not always stabilising (Fig. 1). An increase in the delay can lead to an expansion of the parameter region where solutions are cyclic. Therefore, an increase in the delay can destabilise the dynamics.

To illustrate this behaviour more clearly, we look at λ–T parameter space, with a fixed value of α. Figure 2 shows that for $p = 0.2$ (black solid line), the boundary between the stable and unstable regions oscillates as the delay increases. As the delay increases, its effect changes between being stabilising and destabilising. In addition, comparison of the $p = 0$ line (dashed) with the $p = 0.2$ curve shows that the effect of DDP alternates between being stabilising and destabilising as the delay changes.

The pattern becomes more complex as the strength of the prophylactic response (p) increases (Fig. 2); the oscillatory pattern of the stability curves becomes more irregular, and there are increasingly elongated extensions of the lower part of the
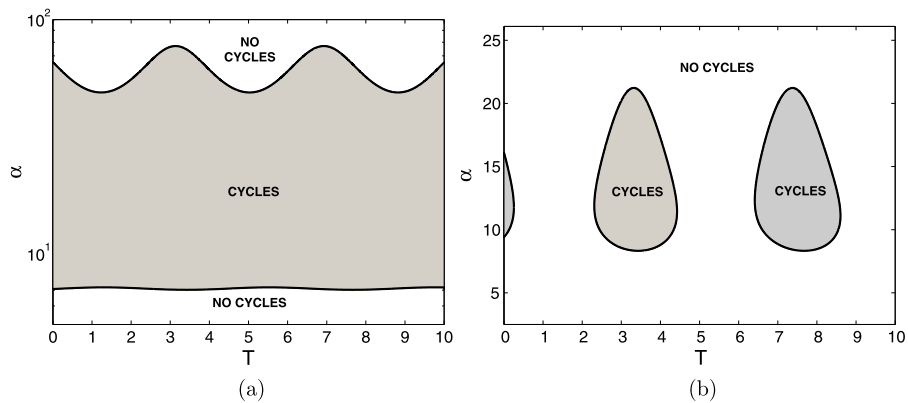
Fig. 2 Stability boundary curves for $p = 0.2$ (*black*), $p = 0.4$ (*dark grey*) and $p = 0.6$ (*pale grey*) in λ–T parameter space. The curve for $p = 0$ (*dashed*) is also shown for comparison. Below the lines, there are no cycles; above the lines, there are cycles. In this figure, $\alpha = 15.5$; the other parameters are as in Fig. 1. Note that the oscillations in the stability boundary are not periodic. These curves are produced using a numerical continuation method (described in Sect. 4) and confirmed through theoretical analysis (Sect. 5)

stability boundary. The population dynamics of the system become more complicated with a longer delay and with a stronger prophylactic response.

Next we look at α–T parameter space, with fixed λ. The results depend on the value of λ. For relatively large λ, the stability boundaries are as shown in Fig. 3(a): there are two boundary curves, with cycles occurring for parameters lying between the curves. In this figure, $\lambda = 5 \times 10^7$. If extended, the stability boundary curves of Fig. 1 would cross the line $\lambda = 5 \times 10^7$ twice. These two crossings correspond to the two stability boundary curves in Fig. 3(a). In contrast, for relatively small λ, the boundaries are as shown in Fig. 3(b), with a series of distinct regions in parameter space in which cycles are generated. The value of λ here is 0.8×10^7. To understand this behaviour, one can observe that in Fig. 1, some stability boundary curves cross the line $\lambda = 0.8 \times 10^7$, while others do not. So for some delays, there are no cycles for any value of α.

It can be seen from Fig. 2 that for certain values of λ there are multiple stability switches as the time delay increases. These are illustrated by the simulations shown in Fig. 4; as the delay increases, the long-term dynamical behaviour alternates between non-cyclic and cyclic. There are also stability switches for certain values of α as the delay increases (Figs. 3(a) and (b)).

Fig. 3 (**a**) Stability boundary curves for $p = 0.2$ in α–T parameter space, for 'large' λ. In this figure, $\lambda = 5 \times 10^7$. There are two curves, and cycles are generated for parameters lying between them. Note that for clarity, a log scale is used for the vertical axis. (**b**) Stability boundary curves for $p = 0.2$ in α–T parameter space, for 'small' λ. In this figure, $\lambda = 0.8 \times 10^7$. In this case, the curves form 'islands', and cycles are generated for parameters within these islands

4 Continuation Method

The numerical technique used to determine the stability boundaries presented in this paper involves tracking when roots of the characteristic equation cross the imaginary axis. If all characteristic roots have negative real parts, then the equilibrium is stable; if the real part is non-negative for any characteristic root, then the equilibrium is unstable.

When there is no delay, we can find the boundary in parameter space dividing stable and unstable behaviours by consideration of the Routh–Hurwitz stability criteria. (With the characteristic equation in the form $z^3 + Az^2 + Bz + C = 0$, cycles occur when $AB - C < 0$; this partitions parameter space.) However, when there is a delay the characteristic equation has an infinite number of roots (eigenvalues) and so can no longer be solved algebraically. Instead, we use a point on the stability curve for $T = 0$ as a starting point for numerical continuation, tracking the passing of eigenvalues across the imaginary axis. This enables us to trace the stability boundary curves through parameter space. Numerical continuation can be performed in any of the parameters p, T, α or λ; a combination is required to produce the various figures presented in this study. Switching beween parameters allows curves to be produced that are not monotonic in any one parameter. As an example, Fig. 3(b) is produced by parameter continuation in α and T. In this case, the curve is not always monotonic in T, and as a result, numerical continuation via increasing T will fail. When this occurs, we switch to numerical continuation in α in order to continue the curve. Although we have written our own numerical code, we comment that there are software packages that are able to trace stability boundaries for delay differential equations, for example DDE-BIFTOOL (Engelborghs et al. 2002; http://twr.cs.kuleuven.be/research/software/delay/ddebiftool.shtml).
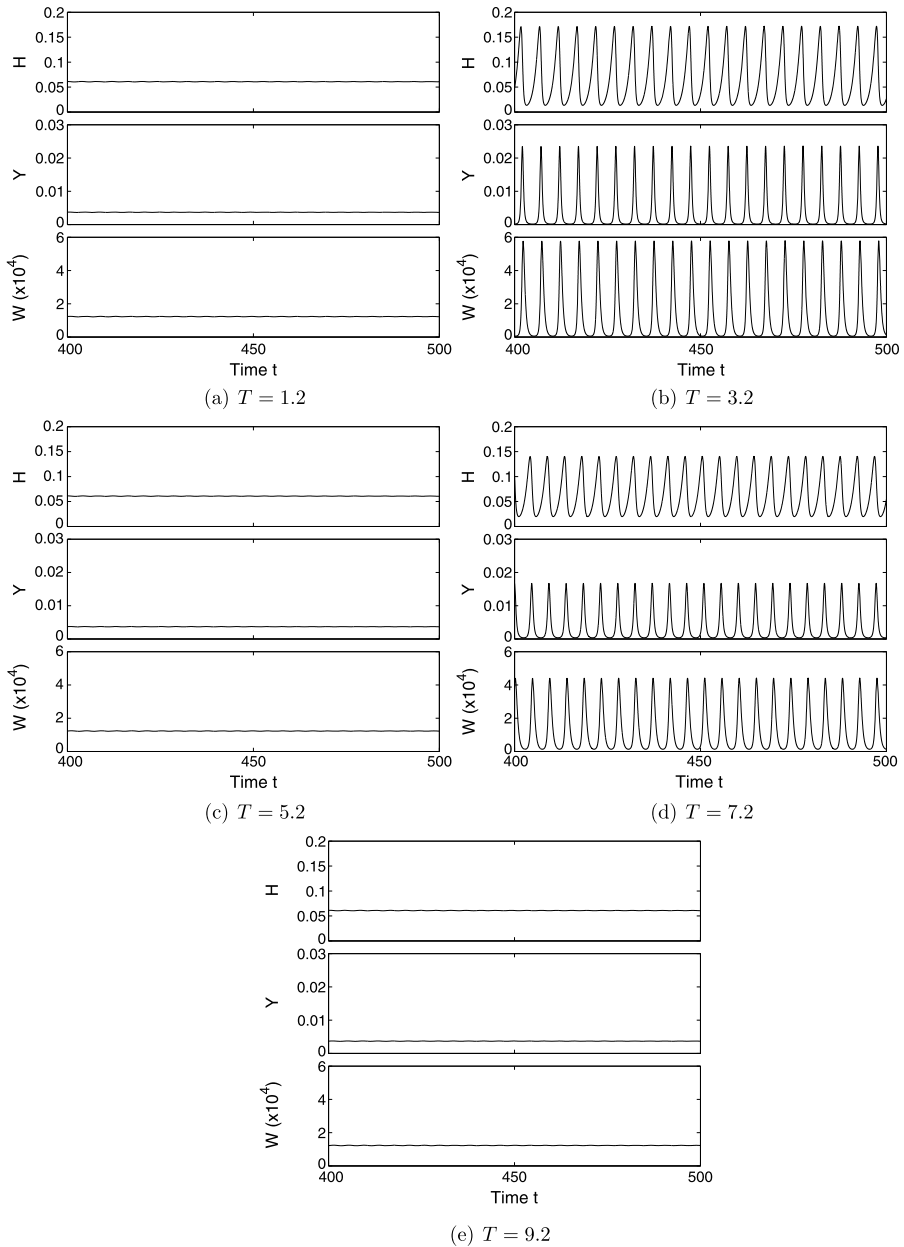
Fig. 4 Numerical simulations of Eqs. (1)–(3) to illustrate the stability switches as the delay T increases. Times series are shown for five different values of T. All other parameter values are the same for all plots, and are as follows: $r = 1$, $K = 1$, $\alpha = 15.5$, $b = 3.3$, $\mu = 3$, $\lambda = 1 \times 10^7$, $p = 0.2$ and $\beta_0 = 0.0001$. The large time dynamical behaviour alternates between cyclic and non-cyclic. These simulations are produced by Matlab (http://www.mathworks.co.uk) using the delay differential equation solver dde23, which is based on an explicit Runge–Kutta $(2, 3)$ pair. Solutions are shown after running for 400 time units to ensure decay of transients

5 Analysis of Stability Switching

General mathematical theory of stability switching in delay differential equations is presented in Kuang's (1993) book, which summarises the work of various previous authors including Mufti (1964) and Cooke and van den Driessche (1986). We now apply this theory to the system (1)–(3). We do not attempt a general survey of behaviour across the entire parameter space: rather, our more modest objective is to show that our numerical results can be confirmed and explained analytically for typical parameters. In particular, we will use as an example case the change in stability with T for $\lambda = 0.6 \times 10^7$ and $p = 0.4$, with other parameters as in Fig. 2.

The characteristic equation of (1)–(3) is

$$C_0 + C_1 E + C_2 E^2 + E^3 - \alpha(\mu + E)\Upsilon e^{-TE} = 0 \qquad (6)$$

where Υ, C_0, C_1 and C_2 depend on the model parameters as follows:

$$\Upsilon = \frac{\beta_0 p}{K} W^*(H^* - Y^*),$$

$$C_0 = \alpha\mu\Gamma + r\left(\frac{2H^*}{K} - 1\right)\left(\Gamma\mu + \alpha\mu + b\mu - \frac{\lambda\Gamma(H^* - Y^*)}{W^*}\right),$$

$$C_1 = r\left(\frac{2H^*}{K} - 1\right)(\mu + \Gamma + \alpha + b) + \Gamma\alpha + \Gamma\mu + \alpha\mu + b\mu - \frac{\lambda\Gamma(H^* - Y^*)}{W^*},$$

$$C_2 = r\left(\frac{2H^*}{K} - 1\right) + \mu + \Gamma + \alpha + b,$$

$$\Gamma = \beta_0\left(1 - \frac{p}{K}H^*\right)W^*.$$

We use the term "stable" to mean that $\mathrm{Re}\, E < 0$ for all eigenvalues E. One special case that we exclude from the outset is $C_0 = \alpha\mu\Upsilon$. This would imply that $E = 0$ is a solution of (6) for all T, so that the steady state is never stable.

At a stability change, an eigenvalue E has zero real part. Setting $E = i\omega$ (with ω real) and equating real and imaginary parts of Eq. (6) gives

$$C_0 - C_2\omega^2 = \Upsilon\alpha\big[\mu\cos(T\omega) + \omega\sin(T\omega)\big] = \Upsilon\alpha\sqrt{\mu^2 + \omega^2}\cos(\phi - \omega T), \quad (7)$$

$$C_1\omega - \omega^3 = \Upsilon\alpha\big[\omega\cos(T\omega) - \mu\sin(T\omega)\big] = \Upsilon\alpha\sqrt{\mu^2 + \omega^2}\sin(\phi - \omega T) \quad (8)$$

where ϕ is defined by $\frac{\mu}{\sqrt{\mu^2+\omega^2}} = \cos\phi$, $\frac{\omega}{\sqrt{\mu^2+\omega^2}} = \sin\phi$, $\phi \in [0, 2\pi)$. The system (7), (8) constitutes two real equations for the two unknowns ω and T, as functions of the various model parameters. An important preliminary observation is that given any solution (ω^*, T^*), $(-\omega^*, T^*)$ is also a solution. Moreover, our assumption $C_0 \neq \alpha\mu\Upsilon$ means that $\omega = 0$ does not satisfy (7), (8). Therefore at a stability change two eigenvalues (a complex conjugate pair) cross the imaginary axis. Henceforth we assume $\omega > 0$ without loss of generality.

Following the standard approach (e.g. Murray 2002, §1.4–1.5), we eliminate T from (7), (8), giving a cubic equation for ω^2:

$$\left(C_0 - C_2\omega^2\right)^2 + \omega^2\left(C_1 - \omega^2\right)^2 = \Upsilon^2\alpha^2\left(\mu^2 + \omega^2\right). \tag{9}$$

This can have between zero and three real positive roots for ω. For our example case there are two real positive roots, $\omega = \omega_1 \equiv 1.485$ and $\omega = \omega_2 \equiv 1.547$, and for the various other biologically realistic parameter sets that we have investigated there are also two distinct real positive roots. For any given root ω, (7) implies that

$$T = \frac{1}{\omega}\cos^{-1}\left(\frac{\mu}{\sqrt{\mu^2 + \omega^2}}\right) - \frac{1}{\omega}\cos^{-1}\left(\frac{C_0 - C_2\omega^2}{\Upsilon\alpha\sqrt{\mu^2 + \omega^2}}\right). \tag{10}$$

Since $\cos^{-1}$ is multi-valued, it follows that for each real value of ω, the corresponding eigenvalue crosses the imaginary axis an infinite number of times as T increases. The difference in T between each crossing is

$$\Delta T = 2\pi/\omega. \tag{11}$$

In order to determine the type of stability change (if any) that occur when an eigenvalue pair crosses the imaginary axis, it is necessary to investigate whether the pair is crossing from the left hand half of the complex plane into the right hand half, or vice versa. A condition for this was derived by Cooke and van den Driessche (1986) and is also given in Kuang's (1993) book. Since both references are a little obscure (especially, Kuang's book is currently out of print), we give a brief summary of the argument. We begin by writing the characteristic equation (6) as

$$P(E) + Q(E)e^{-ET} = 0; \tag{12}$$

here $P(E) = C_0 + C_1 E + C_2 E^2 + E^3$ and $Q(E) = -\alpha(\mu + E)\Upsilon$. We seek to calculate

$$S = \text{sign}\left(\frac{\mathrm{d}}{\mathrm{d}T}\left(\text{Re } E(T)\right)\Big|_{E=\mathrm{i}\omega}\right) = \text{sign}\left[\text{Re}\left(\frac{\mathrm{d}E(T)}{\mathrm{d}T}\Big|_{E=\mathrm{i}\omega}\right)\right].$$

Differentiating (12) with respect to T yields

$$\frac{\mathrm{d}E}{\mathrm{d}T} = \frac{EQ(E)}{P'(E)e^{ET} + Q'(E) - TQ(E)} = \left(-\frac{P'(E)}{EP(E)} + \frac{Q'(E)}{EQ(E)} - \frac{T}{E}\right)^{-1} \tag{13}$$

using (12). Hence

$$S = \text{sign}\left(\text{Re}\left(\frac{\mathrm{d}E}{\mathrm{d}T}\right)^{-1}\Big|_{E=\mathrm{i}\omega}\right)$$

$$= \text{sign Re}\left[-\frac{P'(\mathrm{i}\omega)}{\mathrm{i}\omega P(\mathrm{i}\omega)} + \frac{Q'(\mathrm{i}\omega)}{\mathrm{i}\omega Q(\mathrm{i}\omega)} - \frac{T}{\mathrm{i}\omega}\right] = \text{sign Im}\left[\frac{Q'(\mathrm{i}\omega)}{Q(\mathrm{i}\omega)} - \frac{P'(\mathrm{i}\omega)}{P(\mathrm{i}\omega)}\right] \tag{14}$$

since T and ω are real and positive.

In terms of the notation used for (12), Eq. (9) is $0 = |P(i\omega)|^2 - |Q(i\omega)|^2 \equiv F(\omega)$. Since our interest in S is only for values of ω that satisfy (9), it follows that

$$S = \text{sign Im}\left[\frac{Q'(i\omega)\overline{Q(i\omega)}}{Q(i\omega)\overline{Q(i\omega)}} - \frac{P'(i\omega)\overline{P(i\omega)}}{P(i\omega)\overline{P(i\omega)}}\right]$$

$$= \text{sign Im}\left[Q'(i\omega)\overline{Q(i\omega)} - P'(i\omega)\overline{P(i\omega)}\right]$$

where overbars denote complex conjugation. Writing $F(\omega) = P(i\omega)\overline{P(i\omega)} - Q(i\omega)\overline{Q(i\omega)}$ and differentiating then yields

$$S = \text{sign}\left[F'(\omega)\right]. \tag{15}$$

This result has two key implications. Firstly, S is independent of the delay value, depending only on ω. We have already commented that for all of the biologically realistic parameter sets we have considered, (9) or equivalently $F(\omega) = 0$ has two simple real roots. The second key implication of (15) is that since $F'(\omega)$ must have an opposite sign at these two roots, one of them corresponds to a complex conjugate pair of eigenvalues crossing the imaginary axis from left to right, while the other corresponds to a crossing from right to left.

To demonstrate these results we consider our example case: $\lambda = 0.6 \times 10^7$, $p = 0.4$, and the other parameters as in Fig. 2. Our discussion is illustrated in Fig. 5. For $T = 0$, there are three eigenvalues: one negative and a complex conjugate pair with negative real parts; the infected steady state is stable. As mentioned previously, Eq. (9) has two real positive roots: $\omega_1 = 1.485$ and $\omega_2 = 1.547$ (correct to three decimal places). Moreover, $F'(\omega_1) < 0$ and $F'(\omega_2) > 0$, so that ω_1 and ω_2 correspond to crossings of the imaginary axis from right to left, and from left to right, respectively. As the delay increases from zero, the steady state (which is stable at $T = 0$) will become unstable at the smallest positive solution of (10) for $\omega = \omega_2$, say $T = T_{2,1}$. At this value of T there is a crossing of the imaginary axis by an eigenvalue pair corresponding to ω_2. As T is increased further, an eigenvalue pair corresponding to ω_1 crosses the imaginary axis, into the left hand half plane, at $T_{1,1}$ say. Now for $T \in (T_{2,1}, T_{1,1})$ there is only one pair of eigenvalues in the right hand half plane. Therefore the steady state becomes stable at $T = T_{1,1}$. There is another switch to instability at $T_{2,2}$, the second smallest positive solution of (10) with $\omega = \omega_2$, and a switch back to stability at $T_{1,2}$. An eigenvalue pair crosses into the right hand half of the complex plane at each switch to instability, and then crosses back into the left hand half plane at the next switch to stability.

This pattern of alternating stability switches does not continue indefinitely: it is finite. The key to understanding this is formula (11), which implies that $\Delta T_1 = 4.231 > \Delta T_2 = 4.062$. Here ΔT_i is the difference in delay values at which there is a stability switch corresponding to ω_i, so that $T_{i,j+1} - T_{i,j} = \Delta T_i$ for all j ($i = 1, 2$). Therefore as T is continually increased, there will eventually be two consecutive stability switches corresponding to $\omega = \omega_2$, with no switch corresponding to $\omega = \omega_1$ between them. At the second of these switches there is already an eigenvalue pair in the right hand half plane, and therefore it is joined by a second eigenvalue pair. The pattern of eigenvalue pair crossings of the imaginary axis at $T_{1,j}$ and $T_{2,j}$ does continue, but
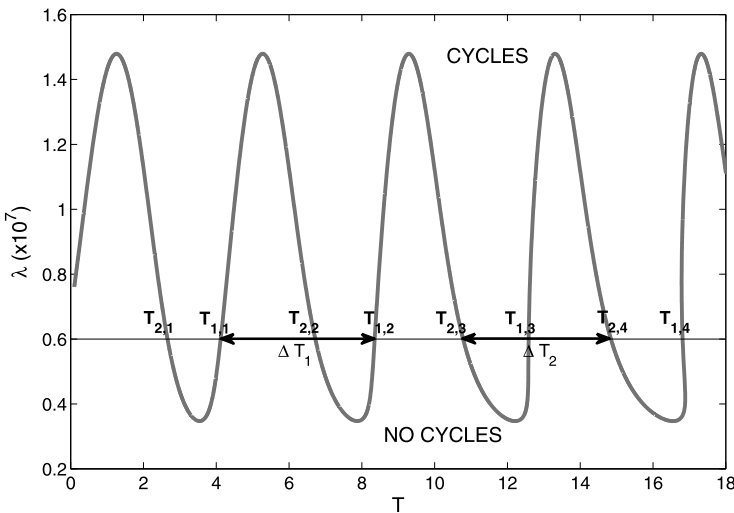
Fig. 5 An example of a stability boundary curve to demonstrate properties of the stability switches. The case shown is for $p = 0.4$. For $\lambda = 0.6 \times 10^7$, there are stability switches between unstable (cycles) and stable (no cycles). The switches from unstable to stable correspond to a crossing of a pair of eigenvalues across the imaginary axis from right to left. The value of ω for these switches is $\omega_1 = 1.485$. The switches from stable to unstable correspond to a crossing of a pair of eigenvalues from left to right. The value of ω for these switches is $\omega_2 = 1.547$. From (11), the difference in T between crossings of the imaginary axis with $\omega = \omega_1$ is $\Delta T_1 = 2\pi/\omega_1 = 4.231$. Similarly, for ω_2, the difference is $\Delta T_2 = 2\pi/\omega_2 = 4.062$. These analytical predictions agree with measurements on the numerically calculated stability boundary illustrated in this figure. Since $\omega_1 < \omega_2$, $\Delta T_1 > \Delta T_2$, and therefore as T increases, there will eventually be two consecutive switches with ω_2. For values of the delay above this, the dynamics will be unstable, as there will always be eigenvalues with positive real part. The other parameter values are as in Fig. 2

now they correspond to an alternation between one and two eigenvalue pairs in the right hand half plane; they are not associated with a change in stability, and the steady state remains unstable.

This underlying behaviour causes the shapes of the stability boundaries shown in Fig. 2. The values of ω_1 and ω_2 depend on λ and other parameters. Figure 6 shows the regions in λ–T parameter space where the dynamics is stable for a fixed value of p ($p = 0.6$). Values of ω_1 and ω_2 become further apart as parameter p increases, implying that there will be fewer stability switches before the dynamics become permanently unstable. This total number of stability switches is parameter dependent, and can be calculated by comparing the sequences $T_{1,j}$ and $T_{2,j}$. For instance, Fig. 7 illustrates the dependence on λ of the number of switches, for $p = 0.6$ and for other parameter values as in Fig. 2.

6 Discussion

In this paper, we have examined the dynamical effects of increasing the length of a time delay in a host–pathogen model incorporating density-dependent prophylaxis (DDP). DDP is the phenomenon of individuals investing more in disease resistance
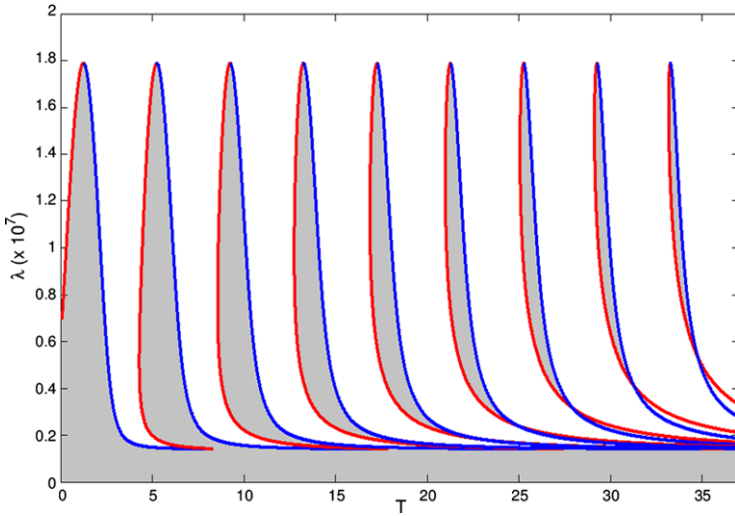
Fig. 6 Regions of different dynamical behaviour in λ–T parameter space for $p = 0.6$. The boundary curve is colour coded according to the direction in which the eigenvalue pair crosses the imaginary axis: *blue* (or *dashed gray*) corresponds to a crossing from left to right; *red* (or *black*) corresponds to a crossing from right to left. The *shading* shows where the dynamics is stable (no cycles) and the non-shaded regions are where the dynamics is unstable (cyclic). In this figure, $\alpha = 15.5$ with the other parameter values as in Fig. 1
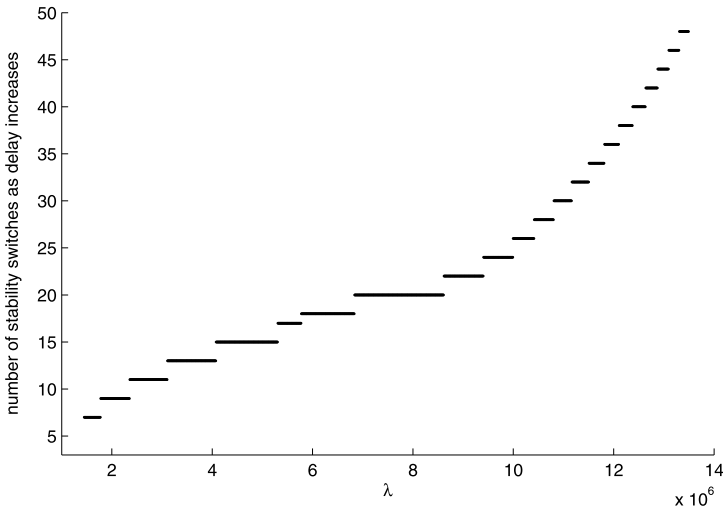
Fig. 7 The number of stability switches that occur as the time delay increases depends on the value of parameter λ, the rate at which an infected host produces infective stages of the pathogen. In this figure, $p = 0.6$ and $\alpha = 15.5$, while the other parameter values are as in Fig. 1

when population densities are high, due to the increased infection potential. Our results provide a rare example of a system of equations with a real-world application in which there are multiple switches between stable (non-cyclic) and unstable (cyclic)

dynamics as the time delay increases. We have demonstrated this in numerical simulations, and we have shown that our numerics agree with analytical theory on stability switching. An important implication of this theory is that the number of switches is finite, with the dynamics eventually becoming unstable. The number of stability switches that occur can be calculated and is dependent on parameters. A consequence of this behaviour is that the regions of stability in parameter space have a complex structure, of the type that we have illustrated via simulation and numerical continuation.

Our findings are consistent with those of Xiao et al. (2009), who find a finite number of stability switches as the delay in host self-regulation increases in a host–pathogen model framework. In this study, we have explained in detail how such stability switches occur and we also have calculated the number of switches for our particular model.

It is useful to consider the length of the time delay relative to the average host life span, which is $1/b$. In a previous study, looking at delays shorter than the average host life span, it was concluded that the effect of DDP on the population dynamics was critically dependent on the delay value (Reynolds et al. 2011). In addition, increasing the delay was found to be stabilising, i.e. it reduced the region in parameter space where solutions were cyclic. In this paper, we find that with longer delays, an increase in the delay can be both destabilising and stabilising.

Many of the delays considered in this paper exceed $1/b$, and therefore correspond to delays spanning generations. This is possible because the environment experienced by a mother can affect the susceptibility of her offspring to disease. For example, in the invertebrate species *Daphnia magna* there is evidence that offspring produced by mothers in crowded conditions are less susceptible to parasites compared to those produced under good conditions (Mitchell and Read 2005).

Our findings highlight the complex interaction between a time delay and population dynamics, with consequent implications for disease dynamics. The stability of this system is critically dependent on the time delay in DDP. There is potential here for empirical investigation: a laboratory experiment designed to estimate this delay for a real system would be highly informative, with an insect species and appropriate virus probably being the most feasible system. Empirical estimation of the delay parameter would enable testable predictions of population dynamics. This would significantly inform the debate on the role of pathogens in driving host population cycles.

References

Anderson, R.M., May, R.M.: Population biology of infectious diseases: part I. Nature **280**, 361–367 (1979)

Anderson, R.M., May, R.M.: The population dynamics of microparasites and their invertebrate hosts. Philos. Trans. R. Soc. Lond. B **291**, 451–524 (1981)

Barnes, A.I., Siva-Jothy, M.T.: Density-dependent prophylaxis in the mealworm beetle *Tenebrio molitor* L. (Coleoptera: Tenebrionidae): cuticular melanization is an indicator of investment in immunity. Proc. R. Soc. Lond. B **267**, 177–182 (2000)

Berezansky, L., Braverman, E., Idels, L.: Nicholson's blowflies differential equations revisited: main results and open problems. Appl. Math. Model. **34**, 1405–1417 (2010)

Bowers, R.G., Begon, M., Hodgkinson, D.E.: Host–pathogen population cycles in forest insects? Lessons from simple models reconsidered. Oikos **67**, 529–538 (1993)

Colijn, C., Mackey, M.C.: A mathematical model of hematopoiesis, I: periodic chronic myelognous leukemia. J. Theor. Biol. **237**, 117–132 (2005)

Cooke, K.L., van den Driessche, P.: On zeroes of some transcendental equations. Funkc. Ekvacioj **29**, 77–90 (1986)

Engelborghs, K., Luzyanina, T., Roose, D.: Numerical bifurcation analysis of delay differential equations using DDE-BIFTOOL. ACM Trans. Math. Softw. **28**, 1–21 (2002)

Fowler, A.C., Kalamangalam, G.P.: The role of the central chemoreceptor in causing periodic breathing. IMA J. Math. Appl. Med. Biol. **17**, 147–167 (2000)

Gurney, W.S.C., Blythe, S.P., Nisbet, R.M.: Nicholson's blowflies revisited. Nature **287**, 17–21 (1980)

Hastings, A.: Age-dependent predation is not a simple process, I: continuous time models. Theor. Popul. Biol. **23**, 347–362 (1983)

Kraaijeveld, A.R., Godfray, H.C.J.: Trade-off between parasitoid resistance and larval competitive ability in *Drosophila melanogaster*. Nature **389**, 278–280 (1997)

Kuang, Y.: Delay Differential Equations with Applications in Population Dynamics. Academic Press, Boston (1993)

Kunimi, Y., Yamada, E.: Relationship between larval phase and susceptibility of the armyworm, *Pseudaletia separata* Walker (Lepidoptera: Noctuidae) to a nuclear polyhedrosis virus and a granulosis virus. Appl. Entomol. Zool. **25**, 289–297 (1990)

Lee, M.S., Hsu, C.S.: On the τ-decomposition method of stability analysis for retarded dynamical systems. SIAM J. Control Optim. **7**, 242–259 (1969)

Mackey, M.C., Milton, J.G.: Dynamical diseases. Ann. N.Y. Acad. Sci. **504**, 16–32 (1987)

Mahaffy, J.M.: A test for stability of linear differential delay equations. Q. Appl. Math. **40**, 193–202 (1982)

May, R.M.: Time-delay versus stability in population models with two and three trophic levels. Ecology **54**, 315–325 (1973)

Mitchell, S.E., Read, A.F.: Poor maternal environment enhances offspring disease resistance in an invertebrate. Proc. R. Soc. Lond. B **272**, 2601–2607 (2005)

Mufti, I.H.: A note on the stability of an equation of third order with time lag. IEEE Trans. Autom. Control **9**, 190–191 (1964)

Murray, J.D.: Mathematical Biology I: An Introduction, 3rd edn. Springer, New York (2002)

Nicholson, A.: An outline of the dynamics of animal populations. Aust. J. Zool. **2**, 9–65 (1954)

Råberg, L., Grahn, M., Hasselquist, D., Svensson, E.: On the adaptive significance of stress-induced immunosuppression. Proc. R. Soc. Lond. B **265**, 1637–1641 (1998)

Reeson, A.F., Wilson, K., Gunn, A., Hails, R.S., Goulson, D.: Baculovirus resistance in the noctuid *Spodoptera exempta* is phenotypically plastic and responds to population density. Proc. R. Soc. Lond. B **265**, 1787–1791 (1998)

Reynolds, J.J.H., White, A., Sherratt, J.A., Boots, M.: The population dynamical consequences of density-dependent prophylaxis. J. Theor. Biol. **288**, 1–8 (2011)

Ruiz-González, M.X., Moret, Y., Brown, M.J.F.: Rapid induction of immune density-dependent prophylaxis in adult social insects. Biol. Lett. **5**, 781–783 (2009)

Ryder, J.J., Webberley, K.M., Boots, M., Knell, R.J.: Measuring the transmission dynamics of a sexually transmitted disease. Proc. Natl. Acad. Sci. USA **102**, 15140–15143 (2005)

Ryder, J.J., Miller, M.R., White, A., Knell, R.J., Boots, M.: Host–parasite population dynamics under combined frequency- and density-dependent transmission. Oikos **116**, 2017–2026 (2007)

White, A., Bowers, R.G., Begon, M.: Population cycles in self-regulated insect pathogen systems: resolving conflicting predictions. Am. Nat. **148**, 220–225 (1996)

Wilson, K., Reeson, A.F.: Density-dependent prophylaxis: evidence from lepidoptera–baculovirus interactions? Ecol. Entomol. **23**, 100–101 (1998)

Wilson, K., Thomas, M.B., Blanford, S., Doggett, M., Simpson, S.J., Moore, S.L.: Coping with crowds: density-dependent disease resistance in desert locusts. Proc. Natl. Acad. Sci. USA **99**, 5471–5475 (2002)

Xiao, Y., Bowers, R.G., Tang, S.: The effect of delayed host self-regulation on host–pathogen population cycles in forest insects. J. Theor. Biol. **258**, 240–249 (2009)